PROCESS DEVELOPMENT FOR LARGE AREA BURIED CONTACT SOLAR CELLS ON MULTICRYSTALLINE SILICON

W. Jooss, P. Fath, E. Bucher
S. Roberts*, T.M. Bruton*
University of Konstanz, Department of Physics
P.O.Box X916, D-78457 Konstanz, Germany Tel.: +49-7531-88-2074, Fax: +49-7531-88-3895
* BP Solar, P.O. Box 191, Sunbury-on-Thames, UK
e-mail: Wolfgang.Jooss@uni-konstanz.de

ABSTRACT: The purpose of this study was the further development of a processing sequence for Buried Contact Solar Cells (BCSC) on multicrystalline silicon (mc-Si). Two different processing sequences were investigated which differ in the effectiveness of rear surface passivation. Common features of both processes are mechanical V-texturing of the front surface for the reduction of reflection losses and a hydrogen plasma treatment for bulk passivation. Front surface passivation is accomplished by LPCVD-SiN_x in both processes. In Process I with a moderate rear surface passivation an average efficiency of 15.4 % was obtained with highest efficiencies of 16.0 % (cell area 156 cm^2). In Process II with an improved rear surface passivation, detailed investigations concerning the temperature dependence of the hydrogen plasma treatment were performed and an optimum process temperature of 450 °C was determined. At this temperature an efficiency gain of 1.0 %abs. was measured as compared to cells without hydrogen passivation on Baysix multicrystalline Si. The best efficiencies obtained within this process were 16.3 % (cell area 156 cm^2).
Keywords: Buried Contacts – 1: Back-Surface-Field – 2: texturisation - 3

1. INTRODUCTION

Crystalline silicon solar cells are playing the major role in the total annual shipment of PV modules world wide (246 MW out of 288 MW) [1]. In the last years, the production of crystalline Si solar cells shifted from single crystals (90 MW (31 %) in 2000) to multicrystalline silicon (155 MW(54 %)). Due to the lower wafer costs, mc-Si is very attractive for solar cell manufacturing in order to reach a significant cost reduction. However, processing of mc-Si is mostly restricted to screen printed solar cells whereas the other major metallisation technique, the Buried Contact Solar Cell BCSC technology, is so far not used for industrial production of mc-Si solar cells. BCSCs are manufactured by BP Solar with an annual output of 9.5 MW in 2000 using Cz-Si. High efficiencies between 16 and 17 % are obtained in the production line (cell area 147.3 cm^2).

Several investigations were made in the past years to develop processing sequences for BCSCs on mc-Si. Efficiencies of 16.7 % (cell area 10.5 cm^2) [2] and 15.8 % (cell area 130 cm^2) [3] have been demonstrated. This paper reports on the further development of a processing sequence for BCSCs on mc-Si. Due to the higher defect densities in these materials which lead to a lower bulk diffusion length L_B of the minority charge carriers, bulk passivation by gettering and hydrogen passivation are effective tools in enhancing L_B. An additional gain in efficiency can be reached by front surface texturing, which is also investigated using mechanical V-texturing.

One major problem in the processing of conventional BCSCs is rear side passivation. Normally, this is accomplished by a thin Al-BSF, where Al is deposited by means of vacuum deposition techniques prior to Al-alloying. Due to an excellent front surface passivation, this strongly affects cell efficiency for bulk diffusion lengths in the range of the wafer thickness. To reduce this limiting effect improved rear side passivation was investigated by enhancing the thickness of the deposited Al-layer by screen printing.

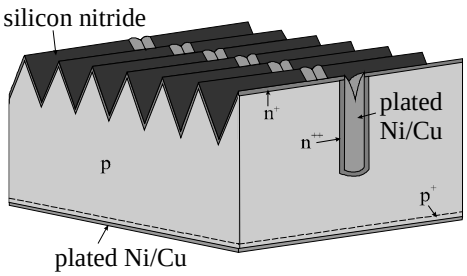

Figure 1: *Schematic illustration of a mechanically V-textured Buried Contact Solar Cell. The contact grooves are perpendicular to the V-texture, silicon nitride serves as ARC and metallisation is performed by electroless plating of Ni and Cu.*

2. SOLAR CELL PROCESSING: PROCESS I

2.1. Process description

A schematic illustration of the device design of a mechanically V-textured solar cell is given in Figure 1. The contact grooves are perpendicular to the V-texture, the front surface is coated by LPCVD-SiN_x as Anti Reflection Coating ARC. The contact grooves and the rear side are metallised by electroless deposition of Ni and Cu.

The investigated sequence for Process I with a thin evaporated Al-BSF is given in Figure 2. This process was already described in more detail in [4]. For our study 45 wafers of Baysix multicrystalline Si from Bayer were taken (starting wafer thickness 330 µm, wafer size 12.5x12.5 cm^2, bulk resistivity $\rho \approx 1\ \Omega$cm). Processing started with mechanical texturing. This was done using a structuring wheel mounted on a DISCO dicing machine with automatic handling system. The texturing angle at the V-groove tips was 80°. The saw damage after V-texturing was removed in a hot solution of sodium hydroxide.

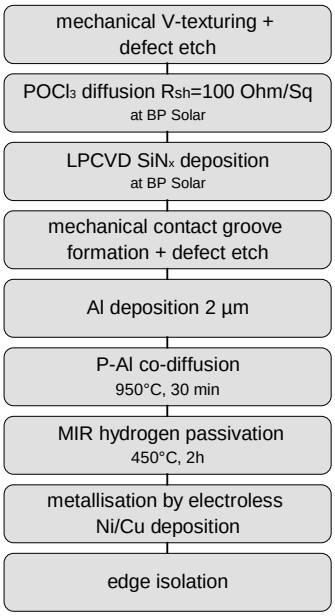

Figure 2: *Applied processing sequence for Process I including mechanical V-texturing. Some process steps were performed in the production line of BP Solar.*

Emitter diffusion (liquid $POCl_3$ source, sheet resistance R_{sheet}≈100 Ω/sq) and Low Pressure CVD deposition of silicon nitride was carried out in the production line of BP Solar España in Madrid. LPCVD SiN_x serves as diffusion barrier during groove diffusion, plating mask during cell metallisation, front surface passivation and ARC. Processing continued at UKN with the formation of the contact grooves by mechanical abrasion: blades with a thickness of 15 µm were mounted on an automatic dicing machine. A finger spacing of 1.4 mm was chosen, and the busbars consisted of 15 contact fingers with a spacing of 100 µm. After removal of the saw damage in the grooves using hot sodium hydroxide, the depth was around 40 µm (measured from the bottom of the V-grooves) and the width around 25 µm. P-Al co-diffusion was applied for the second heavy emitter diffusion in the front grooves and the formation of the Al-BSF by alloying. Al was deposited by electron beam evaporation with a thickness of 2 µm prior to co-diffusion. Emitter sheet resistance was 10 Ω/sqr at the diffusion temperature of 950 °C for 30 min. Besides the reduction of high temperature furnace steps, it was shown, that co-diffusion leads to an enhancement of the bulk diffusion length L_B due to gettering [4]. An additional enhancement of L_B can be achieved by a hydrogen plasma treatment. This was performed in a Microwave Induced Remote Hydrogen Plasma (MIRHP) reactor, which is described in [5]. In previous experiments [4] the optimum passivation temperature of 450 °C was determined for Process I on Baysix material. The passivation time was chosen to be 120 min. Cell metallisation was done by electroless deposition of a thin layer of Ni followed by a thick layer of electroless Cu. In this process the front grooves as well as the Al-Si eutectic on the rear side are metallised in the same process. Edge isolation in industrial production is generally done as the last process step by laser cutting and cleaving. The cut is done at a width of about 1 mm from the edge of the solar cell [6], therefore removing about 3 % of the wafer area. In this work edge isolation was carried out by mechanical abrasion using 150 µm wide dicing blades. The cut was performed close to the wafer edge so the removed wafer material was below 0.5 % of the total cell area.

Table I: *Cell parameters of solar cells manufactured with Process I measured at BP Solar Espana. The best solar cell was tabbed and measured at UKN. Cell area 156 cm².*

	V_{oc} [mV]	J_{sc} [mA/cm²]	FF [%]	η [%]
aver. 45 cells	595	34.7	74.6	15.4
best	601	34.4	77.5	16.0

2.2. Solar cell results

First, the solar cells were characterised by their illuminated IV-parameters. The average efficiency in the batch of 45 solar cells was 15.4 % (measured at BP Solar, busbars not tabbed, see table I). The best solar cell in this experiment reached an efficiency of 16.0 % after busbar tabbing as measured at UKN. For further characterisation the dark IV and J_{sc}-V_{oc} curves were measured to determine the parameters within the Two-Diode-Model. The extracted parameters after fitting of the curve are the following: J_{01}=1.9x10^{-12} A/cm², J_{02}=5.2x10^{-8} A/cm², R_{sh}=12000 Ωcm² and R_s=0.55 Ωcm². The obtained series resistance R_s is a very good value for a large area solar cell and therefore indicates the high quality of this metallisation technique with low contact resistivity and highly conducting fingers. Also the shading loss due to the front grid was below 5 %. The fill factor is therefore not strongly affected by the series resistance but rather due to a moderate saturation current of the second diode. It is not clear whether this is due to intrinsic properties of mc-Si with defects within the space charge region. In contrast to other processes (as for example firing-through silicon nitride in the processing of screen printed solar cells) the hydrogen in-diffusion occurs from the rear side of the solar cell. Therefore the atoms have a long diffusion path to the front side space charge region. Certainly the enlargement of the surface area due to the macroscopic V-texturing by a factor of around 1.5 also increases the saturation current density.

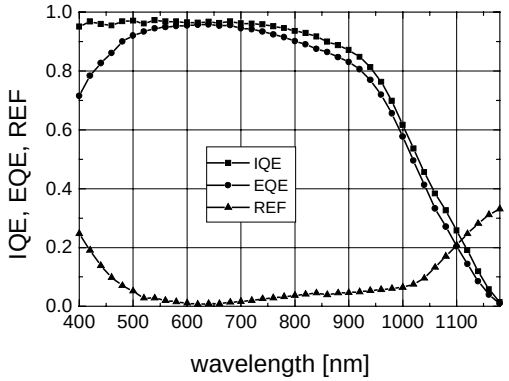

Figure 3: *Internal Quantum Efficiency IQE, External Quantum Efficiency EQE and reflectivity of mechanically V-textured solar cell with Process I.*

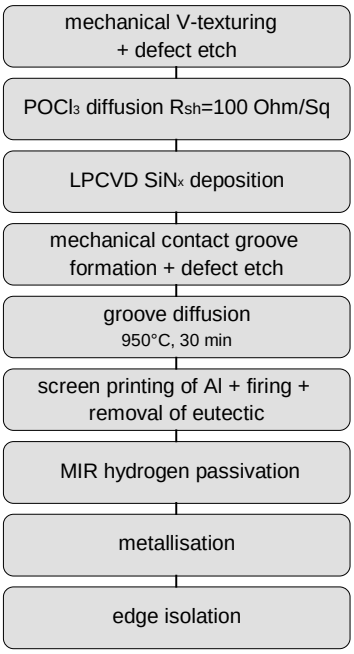

Figure 4: *Applied processing sequence for Process II which includes enhanced rear surface passivation by a screen printed Al-BSF.*

For further characterisation the Internal Quantum Efficiency IQE and External Quantum Efficiency EQE were determined from the measurement of the spectral response and reflectivity. The obtained IQE, EQE and reflectivity of the best solar cell are given in Figure 3. The high IQE in the short wavelength range indicates the high quality of the collecting emitter in conjunction with the surface passivation by LPCVD-SiN_x. From a spectral analysis it can be concluded that the bulk diffusion length is in the range of 230 to 250 µm. Therefore L_B is close to the device thickness and rear side passivation is getting more important. The rear surface recombination velocity S_r of the Al-BSF is mainly determined by the thickness of the deposited Al-layer and the alloying temperature. In our case (2 µm Al, 950 °C), S_r is in the range of several thousand cm/s. Therefore reducing S_r will enhance J_{sc} and V_{oc} for mc-Si material with these diffusion lengths.

In addition to BSFs several other techniques are investigated for rear side passivation; for example floating junction and dielectric passivation. However, floating junction passivation seems difficult to accomplish by maintaining the simple processing sequence of industrial type processes. Dielectric passivation requires better surface recombination velocities than S_r of the thin evaporated Al-BSF within Process I. The dielectric which would be best suited for this work is LPCVD-SiN_x which can be deposited in the same process on front and rear. However, the LPCVD SiN_x presently used at UKN was optimised for good front surface passivation and S_r is higher than that of the thin evaporated Al-BSF. Therefore the easiest way to reduce S_r is to enhance the thickness of the Al layer. In this study we have used screen printing rather than evaporating a thicker layer.

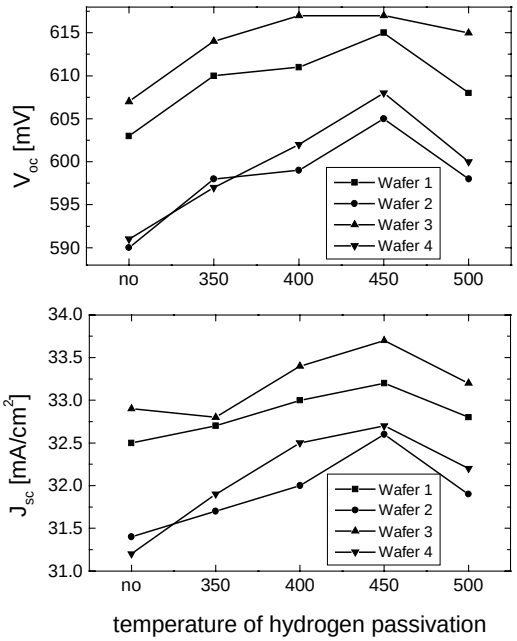

Figure 5: *V_{oc} and J_{sc} of four different 5x5 cm^2 solar cells cut from neighbouring 12.5x12.5 cm^2 wafers. These cells were subjected to hydrogen plasma passivation at different temperatures. Also unpassivated wafers were processed for reference.*

3. SOLAR CELL PROCESSING: PROCESS II

3.1. Processing sequence

The processing sequence is given in Figure 4. The co-diffusion of Process I was replaced by separate diffusion of the contact grooves and the Al-BSF formation. After groove diffusion (950 °C, 30 min, R_{sheet}=10 Ω/sqr), the P-glass was removed in HF. An Al-containing paste was deposited on the rear by screen printing and was fired in a belt furnace.

However, when screen printed Al is used in the processing of buried contact solar cells, problems occur. One problem is the nature of the rear contact after firing, i.e. it is very porous. Since the electroless plating sequence of BCSCs requires wet chemical etching and deposition steps, the chemicals will be soaked in the Al rear contact matrix and will possibly etch it. Therefore, the Al paste has to be removed before plating or has to be protected by a mask. In this study the Al rear contact was removed in a solution of HCl, leaving the Al-doped p^+-region on the rear. Additionally, whereas the initiation of Ni plating on the Al-Si eutectic was not a problem in Process I, Ni deposition did not occur on the p^+-region in Process II. Therefore a thin layer of Al was deposited by electron beam evaporation prior to plating which served as a seeding layer during electroless plating.

3.2. Hydrogen passivation

For Process II also detailed investigations were carried out for the hydrogen passivation step in the MIRHP-reactor, similar to the ones presented for Process I [4]. Different temperatures between 350 °C and 500 °C were chosen at a passivation time of 120 min. The experiment was performed on neighbouring Baysix wafers from Bayer and Eurosil wafers from Eurosolare with an initial wafer

size of 12.5x12.5 cm^2. Before hydrogen plasma passivation the wafers were cut into four pieces with a size of 5x5 cm^2. For reference solar cells were also processed without hydrogen passivation. J_{sc} and V_{oc} for the four cells from each wafer are illustrated in Figure 5 for Baysix material for the different temperatures of the passivation step. As can be seen, the optimum temperature for hydrogen passivation is 450 °C. The beneficial effect of hydrogen passivation is also more pronounced for the wafers with a lower V_{oc} and J_{sc} without hydrogen treatment (wafer 2 and wafer 4). This suggests that hydrogen passivation can narrow the efficiency distribution during solar cell processing. On average the gain due to MIRHP as compared to cells without passivation was ΔV_{oc}=13 mV, ΔJsc=1.1 mA/cm^2 and $\Delta\eta$=1 %abs. The same temperature dependence was observed for Eurosil with an optimum passivation temperature of 450 °C, but the gain was lower (ΔV_{oc}=5 mV, ΔJsc=0.5 mA/cm^2 and $\Delta\eta$=0.5 %abs.).

3.3. High efficiency solar cell processing

After the evolution of a processing sequence with improved rear side passivation, this process was applied for the fabrication of highly efficient solar cells. Besides Baysix mc-Si material, (starting wafer thickness 330 µm, wafer size 12.5x12.5 cm^2, bulk resistivity $\rho\approx1$ Ωcm) also mc-Si from a different supplier was included (starting wafer thickness 350 µm, wafer size 12.5x12.5 cm^2, bulk resistivity $\rho\approx0.5$ Ωcm). For a further increase in J_{sc} due to reduced reflection losses, mechanical V-texturing was performed using a single blade approach. The main advantage as compared to wheel texturing is a reduced curvature within the V-grooves and also a different texturing angle was chosen. The results of the illuminated IV-characteristics are given in Table II. A high efficiency of 16.3 % was reached for the V-textured cell using the material of the alternative supplier. This is to our knowledge the highest efficiency obtained on large area BCSCs. Also a good V_{oc} of 628 mV was measured on the planar cell, which also indicates the enhanced rear surface passivation within Process II. Low fill factors prevented higher efficiencies on the V-textured cells. This was caused by rather high J_{02} and also by a poor adhesion of the rear contact due to non-optimised plating of the p^+-region. From the best V-textured cell the IQE and EQE as well as reflectivity were determined and are shown in Figure 6. The improved IQE in the long wavelength range also indicates the enhanced rear surface passivation in Process II. From a spectral analysis the effective bulk diffusion length L_{eff} was determined to about 300 to 330 µm. For a further improvement in cell efficiency, future experiments will address the problems of rear side metallisation in Process II.

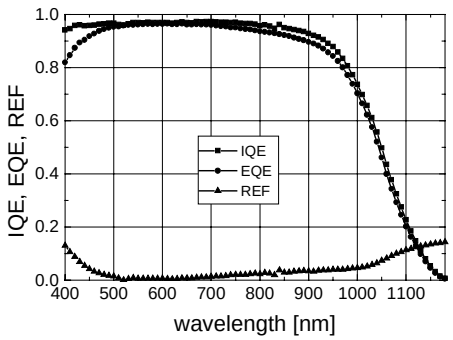

Figure 6: *Internal Quantum Efficiency IQE, External Quantum Efficiency EQE and reflectivity of best mechanically V-textured solar cell within Process II.*

Table I: *IV-parameters of solar cells manufactured with Process II with planar as well as V-textured front surface. V-texturing was done with the Single Blade SB approach. Mc-Si from Bayer and from an alternative source were used in this experiment. Cell area 156 cm^2.*

	V_{oc} [mV]	J_{sc} [mA/cm^2]	FF [%]	η [%]
Bayer, SB	600	35.5	74.8	16.0
Alter., planar	628	32.8	77.2	15.9
Alter., SB	614	35.5	74.8	16.3

4. CONCLUSION

In this study two different processing sequences were investigated for BCSCs on mc-Si. In both processes mechanical V-texturing for the reduction of reflection losses and bulk passivation by a hydrogen plasma treatment is incorporated. The difference between the two processes is the rear surface passivation, with a moderate passivation in Process I (thin evaporated Al-BSF) and an improved one in Process II (thick screen printed Al-BSF). In Process I an average efficiency of 15.4 % was reached in a batch of 45 cells with the best efficiency of 16.0 %. For Process II the optimum temperature of 450 °C for the MIR hydrogen plasma passivation was determined with an average gain in efficiency of 1.0 %abs. on Baysix and 0.5 %abs. on Eurosil. The best efficiency in Process II reached 16.3 % (cell area 156 cm^2), which is to our knowledge the highest efficiency reported for large area BCSCs on mc-Si. Unfortunately, even higher efficiencies were prevented by a poor adhesion of the rear contact and a high J_{02}.

5. ACKNOWLEDGEMENTS

We would like to thank M. Keil for technical assistance during solar cell processing, C. Gerhards and A. Fischer for support during mechanical V-texturing, and B. Fischer for fruitful discussions. This work was supported within the JOULE project by the European Commission under contract number JOR-CT98-0226 (ASCEMUS- Advanced Solar Cells and Modules from Multicrystalline Silicon).

6. REFERENCES

[1] PV News, **20** (3), March 2001

[2] J.C. Zolper, S. Narayanan, S.R. Wenham, M.A. Green, Appl. Phys. Lett. **55** (1989) 2363

[3] S. Narayanan, J. Wohlgemuth, J. Creager, S. Roncin, M. Perry, Proc. 12th EC PVSEC (1994) 740

[4] W. Jooss, M. Spiegel, P. Fath, E. Bucher, S. Roberts, T.M. Bruton, Proc. 16th EC PVSEC Glasgow (2000) 1169

[5] M. Spiegel, P. Fath, K. Peter, B. Buck, G. Willeke, E. Bucher, Proc. 13th EC PVSEC Nice (1995) 421

[6] T.M. Bruton, K.C. Heasman, J.P Nagle, D.W. Cunningham, N.B. Mason, R. Russell, M.A. Balbuena, Proc. 12th EC PVSEC (1994) 761